

Simultaneous Crystallization of Isotactic and Syndiotactic Sequences of Polypropylene

Angiolina Comotti,[†] Roberto Simonutti,[†] Silvia Bracco,[†] Luca Castellani,[‡] and Piero Sozzani^{*,†}

Dipartimento di Scienza dei Materiali, Università di Milano–Bicocca, Via R. Cozzi 53, I-20125 Milano, Italy, and Pirelli Cavi e Sistemi S.p.A., Viale Sarca 222, 20126 Milano, Italy

Received December 18, 2000; Revised Manuscript Received April 12, 2001

ABSTRACT: Polypropylene samples containing 45% isotactic and 20% syndiotactic pentads were characterized by calorimetry and solid-state NMR. Iso- and syndio-sequences are able to crystallize in the same sample to form a complex mixture of several allomorphs: monoclinic α_2 phase together with disordered α phases for isotactic and extended chain together with helix forms for syndiotactic stereosequences. The fraction of each phase was established quantitatively, due to the limited overlapping of the signals at room and high temperature. The partition of stereosequences between the amorphous and crystalline phases was determined at room and high temperature. The distribution of the stereosequences in the amorphous phase was established at high temperature at the pentad level; thus, it was possible to determine the stereosequences already crystallized at that temperature. Hydrogen spin–lattice relaxation times in the rotating frame, measured under spin diffusion conditions, demonstrate the segregation of iso- and syndiotactic crystallites and the intimacy of the phases of the same tacticity.

Introduction

The first crystal structure of α isotactic polypropylene was obtained in the 1950s,¹ and, since then, evidence provided by XRD, calorimetric analysis (DSC), solid-state NMR, and morphological observations has led to the discovery of the structure of several other allomorphs of polypropylene. The variety of the stereochemical distributions now available together with more perfect homotactic samples has helped in the understanding of the microstructure vs crystal structure relationship and the role of stereochemical defects in the crystal arrangement.² The macroscopic properties of materials (mechanical, insulating, etc.) can be modulated on the basis of this knowledge. The fascinating picture of the polypropylene proteiform structure has been outlined by quite vast literature, which has been enriched by many recent contributions. The characterization of the allomorphs of isotactic and syndiotactic polypropylene is given in the following papers and in the references therein reported: (i) isotactic polypropylene in the α form;^{3–9} (ii) isotactic polypropylene in the β form;^{10–13} (iii) isotactic polypropylene in the γ form;^{14–18} (iv) syndiotactic polypropylene in the helix form I;^{19–22} (v) syndiotactic polypropylene in the helix form II;^{23,24} (vi) syndiotactic polypropylene in the stretched form III;^{25–31} (vii) syndiotactic polypropylene in the Chatani form IV.^{28,32,33}

Solid-state NMR spectroscopy has contributed substantially to the identification of the allomorphs of polypropylene; this is because of the marked dependence of chemical shift on polymer chain conformations. Also, crystal packing can be sometimes identified.³⁴ Moreover, a variety of NMR experiments can give an insight into the structure of crystalline (CR) interphases and non-crystalline (NC) phases.^{35,36} At the present stage, we have found ourselves in a favorable position to understand complex systems made by polypropylene contain-

ing isotactic and syndiotactic stereosequences, each able to crystallize in more than one phase. We are also able to describe which stereosequences segregate in the amorphous phase and cannot crystallize at a certain temperature. The conformations and the motion properties of the chains in the multiple phases are reported.

Experimental Section

Materials. The polypropylene used was supplied by Huntsman (Rexene Resins) and is synthesized by a solid supported catalyst of titanium tetrachloride and magnesium chloride. The catalyst was prepared in the absence of electron donors. The use of highly active stereospecific catalysts resulted in the production of prevalently isotactic homopolymers that do not require purification or removal of the atactic or low crystalline polymer. This procedure provides a high molecular weight amorphous propylene homopolymer that has elastic properties (EP Pat. No. 0475306 B1). A diethyl ether soluble fraction of the polymer has no isotactic crystallinity. The melt viscosity of the sample is greater than 200 000 cps at 190 °C. The microstructure was determined by ¹³C NMR at 100 °C in 1,2,4-trichlorobenzene solution at 100.6 MHz (recorded on a Bruker DMX400) and showed the following pentad fractions: *mmmm* = 0.45, *mmmr* = 0.08, *rmmr* = 0.01, *rrmm* = 0.11, *rrmr* + *mrrm* = 0.05, *rrrr* = 0.20, *rrrm* = 0.06, *mrrm* = 0.04. Homosequences prevail, indicating a distribution of the stereosequences far from being Bernoullian and showing the blockiness of the microstructure. This provided the base samples that were subjected to different thermal treatments and will be identified as follows: (a) The “PP” sample was obtained by thermal treatment at 200 °C for 5 min followed by cooling to 120 °C in 40 min and further cooling to room temperature in 20 min. (b) The “annealed PP” sample was a base sample heated to 200 °C and held at this temperature for 15 min to suppress the memory of thermal history, and it was then cooled to 20 °C (cooling rate of 5 °C/min) and heated a second time to 166 °C in three steps: 5 °C/min from room temperature to 130 °C, 1 °C/min from 130 to 160 °C, and 0.2 °C/min from 160 to 166 °C. At the end the sample underwent cooling from 166 to 20 °C at a rate of 10 °C/min. (c) The “rapidly cooled PP” sample was a base sample melted, kept at 190 °C for 2 h, and then cooled at 10 °C/min.

DSC Analysis. We performed the calorimetric analysis (DSC) with a Mettler Toledo instrument equipped with N₂ low-

[†] Università di Milano–Bicocca.

[‡] Pirelli Cavi e Sistemi S.p.A.

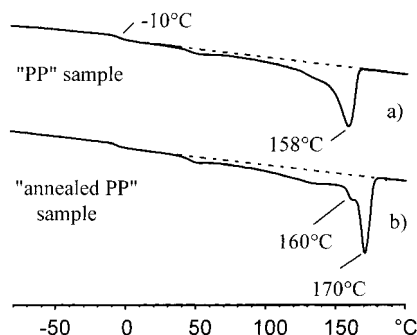


Figure 1. DSC thermograms from -80 to 200 $^{\circ}\text{C}$: (a) "PP" sample; (b) "annealed PP" sample. The heating rate is 10 $^{\circ}\text{C}/\text{min}$.

temperature apparatus. The experiments were run from -100 to 200 $^{\circ}\text{C}$ for all the samples with a heating rate of 10 $^{\circ}\text{C}/\text{min}$. The sample weight from the DSC measurements is typically 8 mg.

Solid-State NMR. ^{13}C MAS NMR spectra were run at 75.4 MHz on a Bruker MSL300 instrument, static field 7.04 T. A MAS Bruker probe head with 7 mm ZrO_2 rotors spinning at a speed of 4 kHz was used. In all the experiments there was a high-power decoupling (DD) field: 90° pulse for proton was 4.7 μs (~ 55 kHz). Single-pulse excitation (SPE) experiments were run using a recycle delay of 4 and 300 s. Cross-polarization (CP) MAS experiments were performed applying a recycle delay of 5 s and a contact time of 1 and 3 ms. The experiments were performed at room temperature, 341 and 361 K.

The ^{13}C T_1 values were obtained using the method developed by Torchia³⁷ (20 spectra were run). Proton relaxation times in the rotating frame $T_{1\rho}(\text{H})$ were measured indirectly, varying the duration of a ^1H spin-lock period before a fixed $^1\text{H} \rightarrow ^{13}\text{C}$ cross-polarization contact time. For each relaxation measurement, 14 spectra were run. The $T_{1\rho}(\text{H})$ and ^{13}C T_1 values were calculated using a nonlinear least-squares fitting routine.

The resolution for carbon was checked on glycine (width at half-height = 23 Hz), and crystalline polyethylene (PE) resonance was taken as the external reference at 32.85 ppm from tetramethylsilane (TMS)³⁸ (literature often reports chemical shift values as referred to PE at 33.63 ppm from TMS).

Results and Discussion

Thermal Behavior. The first heating trace of the "PP" sample (Figure 1a) shows the glass transition at -10 $^{\circ}\text{C}$ and a major endotherm peak at 158 $^{\circ}\text{C}$. The endotherm peak is preceded by a broad shoulder extended over a wide temperature range starting from about 35 $^{\circ}\text{C}$, induced by the complex microstructure of the sample. In this range the thermogram exhibits a small peak at about 50 $^{\circ}\text{C}$ that disappears after melting and 10 $^{\circ}\text{C}/\text{min}$ cooling. The peak at 50 $^{\circ}\text{C}$ is due to the long-term annealing at room temperature. During the cooling treatment crystallization occurs at 112 $^{\circ}\text{C}$, as observed by Lotz for isotactic polypropylene crystallizing from the melt.⁴ Apparently, the sample contains large amounts of low melting species formed by low molecular weight chains, defective microstructures, and less stable crystal forms of iso- and syndio-sequences, as later discussed. The overall melting enthalpy is about 70 J/g. A crystalline fraction of 0.32 can be estimated³⁹ taking into account the melting enthalpy of a totally crystalline isotactic polypropylene. The crystallinity is underestimated, considering that the low specific enthalpy of ill-formed crystallites should be taken into account.

The "annealed PP" sample shows a higher melting peak at 170 $^{\circ}\text{C}$ (Figure 1b). The thermal annealing from 160 to 166 $^{\circ}\text{C}$ (heating rate of 0.2 $^{\circ}\text{C}/\text{min}$) induces the crystallization of high melting lamellae. As observed in

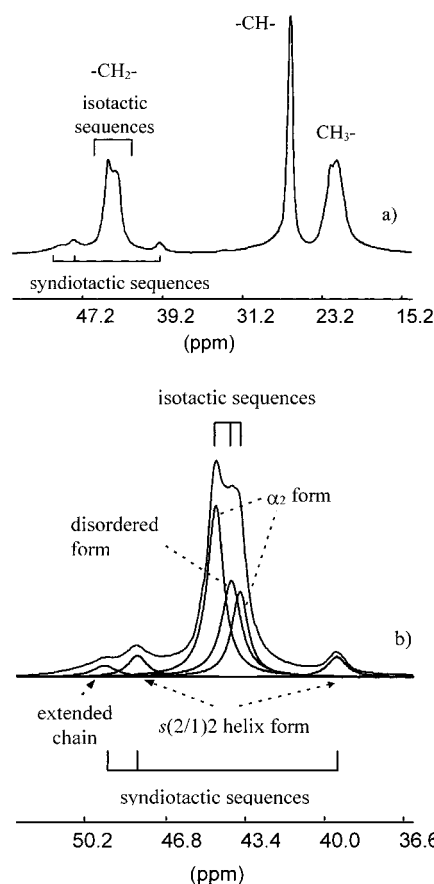


Figure 2. ^{13}C CP MAS NMR spectrum of (a) "PP" sample with a contact time of 1 ms performed at room temperature (full spectrum) and (b) methylene region of the spectrum. The deconvolution of the signals is performed by Lorentzian line shapes. The most intense peaks correspond to the isotactic sequences: the α_2 form is simulated by considering two peaks with the same line width that reproduce an intensity ratio of $2:1$. The central third peak is assigned to the α disordered form (α_d). The syndiotactic helix form is simulated by two peaks with an intensity ratio of $1:1$.

the literature, the thermal treatment at 166 $^{\circ}\text{C}$, which takes place in a partially molten state, gives rise also to a peak at lower temperature, detected as a shoulder at about 160 $^{\circ}\text{C}$.⁴

Identification of Crystalline and Amorphous Phases. Solid-state NMR spectroscopy is one of the most powerful techniques to describe the amorphous phase and the different allomorphs; therefore, it has been applied to analyze samples containing both isotactic^{6,13} and syndiotactic stereosequences of polypropylene.^{16,21,22,27-31}

^{13}C MAS NMR spectra with cross-polarization (CP) and without CP were performed at variable temperatures. The CP technique enhances the rigid and crystalline phases; instead, the SPE sequence enhances the amorphous phases when the spectrum is run with short recycle delays. Long recycle delays give rise to quantitative spectra. The ^{13}C CP MAS NMR spectrum of the "PP" sample (Figure 2) shows a multiplicity of signals for each carbon unit, mainly due to the different crystalline phases. In the methylene region we can recognize two main signals at 43.8 and 44.7 ppm associated with the isotactic polymer.

The pure isotactic polymer forms allomorphs (α , β , γ , and smectic) having the 3_1 helical conformation but differing in the crystal packing. The 3_1 helical conformation is formed when the main chain assumes a strict

alternation of *trans* (*t*) and *gauche* (*g*) conformations (*tg*)_n. Thus, taking into account the helix symmetry of the chain, each carbon of the monomer unit would produce one signal; if splitting is present, it is due to crystal packing, as observed in the methylene region of Figure 2b. Considering the crystal cell of the α form, an intensity ratio of 2:1 would be expected. In our spectrum the ratio is not shown because the upfield signal is too intense, as already observed in refs 8 and 35. However, our interpretation differs from that of Caldas⁸ since we interpret the spectrum as an overlapping of the two signals (2:1 intensity ratio) onto a further signal at 44.0 ppm (Figure 2b). We assign this signal to more disordered phases that lead to the equivalence of each type of carbon in the unit cell. Gomez et al.¹³ reported that the chemical shift of the β and smectic forms partially overlap the upfield signal of the α form. However, in our case X-ray diffraction patterns give no evidence of the presence of β or smectic forms. Disordered modifications of the α form have been described in the literature:⁷ in addition to the highly ordered α phase (called α_2 phase) with $P2_1/c$ space group, an α_1 phase with $C2/c$ space group was proposed. The latter phase includes the disorder of chain directionality. The existence of the "more disordered" α_1 -phase was taken into account by VanderHart and Manderlkern³⁵ for the interpretation of the NMR line shapes of isotactic polypropylenes subjected to different thermal histories. We support this interpretation, assigning the resonance at 44.0 ppm to disordered α phases (hereafter called α_d), as further demonstrated for the other samples. These phases include, as the "more disordered" structure, the α_1 phase proposed on the basis of XRD results.⁷

In the methylene spectrum we can also recognize three minor signals at 49.4, 48.0, and 39.5 ppm, clearly showing the crystallization of the syndiotactic sequences (Figure 2). The methylene signals are very sensitive to conformations explored by syndiotactic stereosequences and resonate over a wide range of chemical shifts (more than 10 ppm), depending on the arrangement of the carbons in the γ position. An upfield shift of 5 ppm is measured⁴⁰ when the observed carbon has, in the γ position, another carbon in a *gauche* conformational relationship. Thus, two units in the *gauche* conformation would generate about 10 ppm upfield shift. In the spectrum the resonances at 48.0 and 39.5 ppm are associated with different methylene conformations, experiencing respectively no γ -*gauche* and two γ -*gauche* effects. The presence of the two signals with 1:1 intensities demonstrates the formation of the *s*(2/1)2 helix typical of I or II crystalline phases.^{21,22} The helix is made up of (*gg**tt*)_n conformational sequences, and there exist two different methylenes at the center of the conformational sequences *txxt* and *gxg*. The crystallization of syndiotactic sequences in the conventional helix form is allowed even if a pentad fraction as low as 0.20 is present. This was made possible because of the stereoblock microstructure, as determined by solution NMR (see Experimental Section). Moreover, the extended-chain form of the syndiotactic sequences characterized by *all-trans* conformations along the main chain is recognized as a minor peak at 49.4 ppm. The formation of extended chain conformation without stretching the sample has already been observed in ref 21. The fraction of chains in this conformation becomes substantial in highly syndiotactic PP, as obtained by metallocene catalyst.^{27,28}

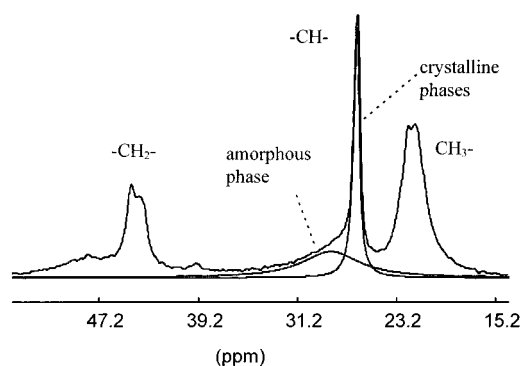


Figure 3. Fully relaxed ^{13}C SPE MAS NMR spectrum of the "PP" sample performed at room temperature. A recycle delay of 300 s is applied. The crystalline and amorphous fractions are obtained by the deconvolution of the methine resonances by Lorentzian line shapes.

The methine carbon lies at the center of *gxxt* conformations in the helix structures of both isotactic and syndiotactic polypropylene, giving rise to one single peak at 26.5 ppm.

The methyl region shows a broad resonance due to the overlapping of several signals originating from isotactic and syndiotactic crystalline forms (Figure 2a). In particular, the α_2 phase of isotactic sequences is known to generate a doublet of 2:1 intensity ratio.^{13,16} The major component is detected at 22.3 ppm in the spectrum of Figure 2a while the minor component overlaps the methyl resonances of syndiotactic *s*(2/1)2 helix form. The syndiotactic extended-chain form contributes to the upfield shoulder of the methyl region.

In the "PP" spectrum we have characterized the crystalline phases, but the signals of the amorphous phase are missing. A ^{13}C SPE MAS NMR spectrum run with long recycle delays (300 s) gives a complete description of the phase content (Figure 3). In fact, the recycle delay of 300 s allows the quantitative detection of both rigid and mobile phases because no carbon nucleus in the "PP" sample has a relaxation time longer than 50 s. In addition to the previous signals, broad resonances due to the amorphous phase appear for methylene and methine at about 47 and 28.5 ppm, respectively. Instead, in the methyl region the amorphous phase is underneath the envelope of the other resonances. The best estimation of the amorphous and crystalline fractions in the fully relaxed spectrum is thus achieved by the deconvolution of the methine spectral region (Figure 3) (all the crystalline phases resonate at the same frequency at 26.5 ppm). A crystalline content of 0.51 can be estimated at room temperature (Table 1). The higher crystalline content measured by NMR, compared to the DSC results (0.32 crystalline fraction), is not surprising considering that NMR recognizes the specific conformation of each crystalline phase also in small and irregular crystals.

The ^{13}C spin-lattice relaxation times shown in Table 1 are about 50 s for crystalline isotactic phases, in agreement with the values reported in the literature for the α phase.¹³ This observation suggests that in the "PP" sample the crystalline phases are well formed, such as to show the same relaxation time as the pure isotactic polymer. The syndiotactic sequences crystallized in the helix form show 46 s ^{13}C relaxation time, in agreement with the value of about 50 s measured by some of the authors for the *s*(2/1)2 helix form of a highly syndiotactic polypropylene sample.²¹

Table 1. Assignments, Relaxation Times, and Amount of the Phases Identified in the "PP" Sample

assignment				ppm	$T_1(^{13}\text{C})$ (s)	$T_{1\rho}(^1\text{H})$ (ms)	content quantitative spectra	
							room temp	361 K
-CH ₂ -	syndiotactic forms	extended chain	49.4	~14	14 ^d	14 ^d	0.02	0
		s(2/1)2	48.0				0.07	0.02
		helix form	39.5					
	isotactic forms	α_2 form	44.7	46 ^e	49 ^f	36 ^c	0.29	0.20
			43.8					
		α_d form ^a	44.0				0.13	0.07
-CH-	amorphous		28.5	48 ^f	35 ^c	35 ^c	0.49	0.71 ^b
	crystalline		26.5				0.51	0.29

^a All arrangements experiencing one γ -gauche effect resonate at this chemical shift. ^b Two peaks are detected. ^c A 0.20 fraction of 6 ms is present. Methyl signals present $T_{1\rho}(^1\text{H})$ of 30 ms. ^d There is also a short relaxing component of 2 ms accounting for 30% likely due to the amorphous phase. ^e There is a short relaxing component of 2 s accounting for 35%. ^f There is a short relaxing component of 7 s accounting for 23%.

The minor fraction of syndiotactic extended chain conformers ($T_1(^{13}\text{C}) \approx 14$ s) may belong to defective parts of a conventional s(2/1)2 helix phase or to small crystals constituted by *all-trans* chains.^{25–28,31} In any case the packing permits a large amount of disorder, giving rise to shorter relaxation times due to increased motions. The amorphous phases show relaxation times of less than 7 s at 298 K. Short relaxation times are consistent with an amorphous polymer well above the glass transition temperature.

The $T_{1\rho}(^1\text{H})$ decays of methylene, methine, and methyl signals for isotactic phases can be resolved into two components with the main component being 35 ms. No difference in value can be detected within the α phases, suggesting a great similarity of the α_2 and α_d phases in terms of mobility or, more probably, a great intimacy of the two phases. The latter possibility takes into account spin diffusion, which locally averages the relaxation time when the abundant nuclei, such as hydrogens, are strongly dipolar-coupled within the crystalline phases.^{41–43}

The $T_{1\rho}(^1\text{H})$ value of 35 ms at the ^1H decoupling field of 15 G is shorter than those reported in the literature for annealed isotactic samples, mainly crystallized in the α forms,^{6,8,44} and is also lower than the ≈ 50 ms value measured for the α phases in the "annealed PP" sample, as shown later. It is likely that the isotactic crystalline phases in the "PP" sample are less ordered; after the annealing process larger and more regular crystals are formed, the defects being segregated in the amorphous phase. The intimate mixing of crystalline phases is a further source of disorder and short relaxation times. Syndiotactic s(2/1)2 helix crystals show about 14 ms for $T_{1\rho}(^1\text{H})$ relaxation times; therefore, the syndiotactic crystals present an independent relaxation mechanism compared to the isotactic crystals. The extended chain syndiotactic conformers belonging to disordered interphases (see $T_1(^{13}\text{C})$ values) are probably intimate with s(2/1)2 helix crystals, $T_{1\rho}(^1\text{H})$ being equal in both phases.

From the $T_{1\rho}(^1\text{H})$ values of 35 and 14 ms for the isotactic and syndiotactic crystals, the phase dimensions, evaluated by a commonly accepted approach, are about 8 and 5 nm, respectively.^{42,43} However, the main contribution to $T_{1\rho}(^1\text{H})$ for the crystalline protons might be not due to the spin diffusion to the noncrystalline protons, but due to intrinsic contributions for motions in the crystalline regions with components in the kilohertz regime.

Short components of less than 6 ms were measured in the analysis of $T_{1\rho}(^1\text{H})$ decays and were assigned to the amorphous phase. For an evaluation of the crystalline phase ratios, we performed a spectrum where the

contribution of the crystalline phases largely prevails by applying the experiment of spin-locking the proton polarization for 3 ms prior to cross-polarizing from the proton to the ^{13}C nuclei for 1 ms. The fractions of the crystalline phase obtained from the deconvolution of the methylene region are reported in Table 1. The internal ratio of the crystalline phases are in agreement with those obtained from the normal CP spectra using a 1 ms CP time. Therefore, with contact times of 1 ms the correct ratio among the crystalline phases is also obtained by the CP technique, because the dynamics of cross-polarization show the same efficiency in all the crystalline phases. Moreover, the content of each crystalline phase of both tactic sequences can be determined from the methylene region of the fully relaxed spectrum.

Variable Temperature Experiments of the "PP" Sample. High-temperature experiments have two effects: (a) they activate greater mobility in the amorphous phase, allowing the collection of narrow and well-defined signals for specific stereosequences, and they allow for the identification of the amorphous phase composition at that temperature; (b) they distinguish between high-melting and defective, low-melting crystals. This results in knowledge of the stereosequences and of those phases that melt in the temperature range from room temperature to 90 °C.

A series of ^{13}C SPE MAS NMR spectra recorded from room temperature to 361 K are shown in Figure 4. In these spectra the amorphous phase is enhanced, the spectra being performed with a short recycle delay (4 s). At room temperature the amorphous phase produces broad signals; at increasing temperatures amorphous phase resonances become narrower and sometimes split due to the resolution of different stereosequences at least at the dyad level (Figure 4c). Narrowing is a common effect for an amorphous polymer 100 deg above its glass transition. Minor signals are due to crystalline phases.

In the methylene and methine region two signals are observed at 361 K for the amorphous phases; the minor one is due to the syndiotactic sequences.

A quantitative spectrum, run at 361 K and long recycle delays (250 s), allows us to establish the amorphous and crystalline fractions at that temperature (Figure 5b). From the deconvolution of the methine peaks an amorphous fraction of 0.71 is measured (Table 1). Comparison with the amorphous content at room temperature (0.49) leads to the conclusion that a crystalline fraction of 0.22 melts from room temperature to 361 K. This phenomenon is in agreement with the melting of species, from room temperature to 361 K, observed in the DSC trace (Figure 1a). The apparent

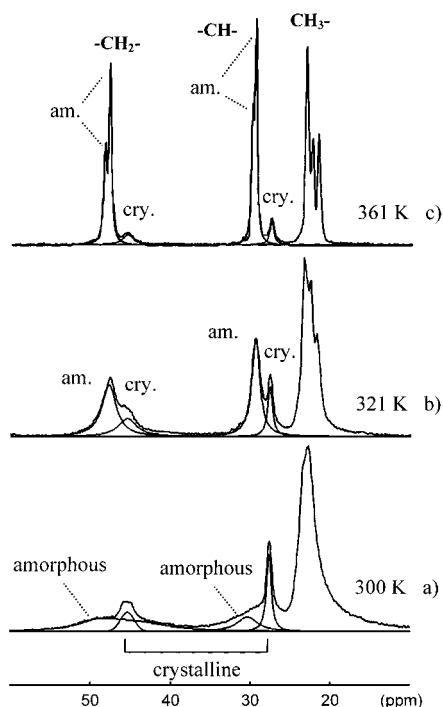


Figure 4. ^{13}C SPE MAS NMR spectra performed at different temperatures from 300 to 361 K. A recycle delay of 4 s is applied. The deconvolution of the signals is performed by Lorentzian line shapes.

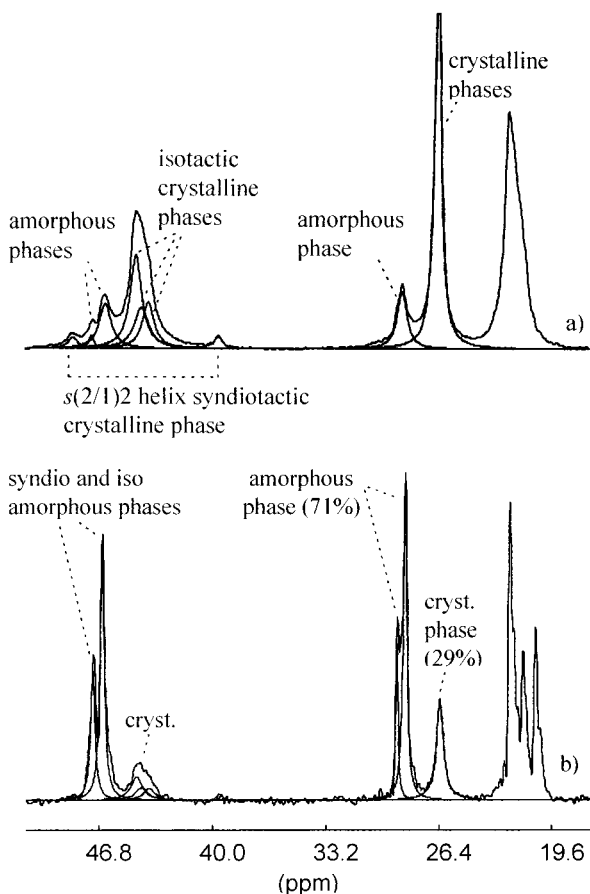


Figure 5. (a) ^{13}C CP MAS NMR spectrum performed at 361 K on the "PP" sample. The contact time of 1 ms is applied. (b) Fully relaxed ^{13}C SPE MAS NMR spectrum performed at 361 K on the "PP" sample. A recycle delay of 300 s is applied.

overestimation of the melted species by NMR, compared to the amount calculated by heat exchanged until 361

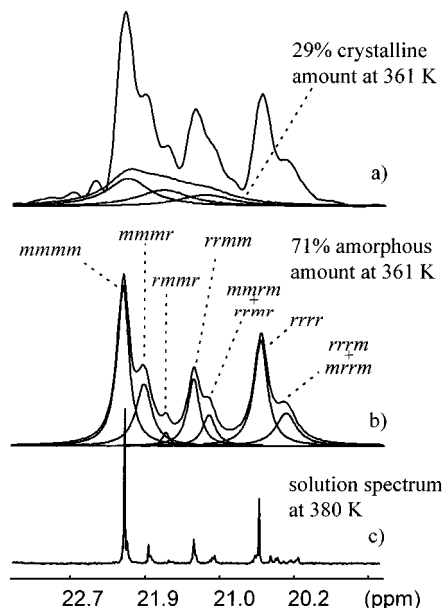


Figure 6. (a) Methyl region of fully relaxed ^{13}C MAS NMR spectrum of "PP" sample. The spectrum is taken at 361 K. The broad line is the envelope of three Lorentzian line shapes corresponding to the peaks of crystalline phases. (b) Methyl resonances of the amorphous phase at 361 K. The resonances are obtained subtracting the broad peak associated with the crystalline phases from the fully relaxed spectrum. (c) Methyl region of the solution NMR spectrum of the "PP" sample taken at 380 K.

K, is due to the long standing time of the sample at high temperatures in the NMR probe and to the low specific enthalpy of the low melting species.

The distribution of the crystallized phases at 361 K can be selectively observed in the CP MAS spectrum, with short mixing times to minimize the amorphous phase (Figure 5a). Moreover, at this temperature there is no overlapping between the crystalline and the amorphous phase resonances, the latter being sharp. Table 1 shows the results of the deconvolution of the methylene region; the amount of crystalline phases at high temperature (column 8) is compared to the amount at room temperature (column 7).

Note the reduction of syndiotactic sequences of the helix form to 0.02 and the disappearance of the extended chain conformation. Thus, most syndiotactic crystals are low melting; this is consistent with our previous observations of short $T_{1\rho}(\text{H})$ values for syndiotactic phases. An analysis of the distribution of the isotactic crystal phases reveals the α_d disordered forms, which are mainly present in the low melting crystals, to be far more sensitive to reduction than the α_2 phase is.

The high resolution obtained at 361 K for the amorphous phase (in the "molten" state) in the quantitative MAS NMR spectrum gives the distribution of the single stereosequences at the pentad level. The methyl region is expanded in Figure 6a. The CP MAS NMR methyl region, weighted for 29% and accounting for the crystalline phases, is subtracted from the methyl region of the quantitative spectrum, giving rise to the amorphous phase spectrum: the deconvoluted signals are highlighted in Figure 6b. Table 2 reports the fractions of the single stereosequences, taking into account a 0.71 total amount of amorphous phase. The composition of the stereosequences in the "molten" state can be compared to the overall microstructure distribution, as determined by solution NMR (Figure 6c). Thus, the composition at

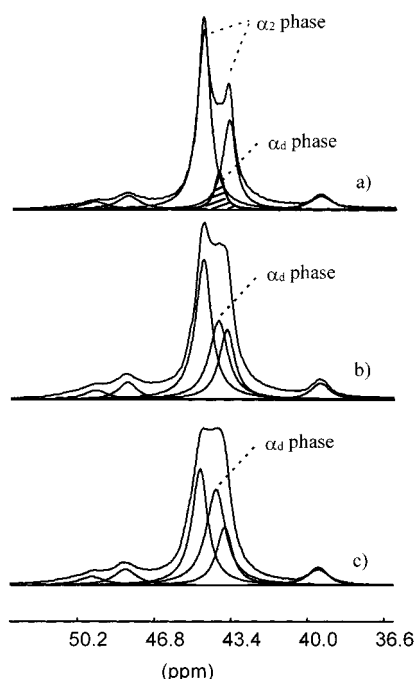


Figure 7. Methylene region of ^{13}C CP MAS NMR spectra performed at room temperature: (a) "annealed PP" sample; (b) "annealed PP" sample; (c) sample heated to the molten state at $190\text{ }^{\circ}\text{C}$ and rapidly cooled. The peaks are deconvoluted by Lorentzian line shapes. The methylene region is deconvoluted as follows: (i) The isotactic crystalline phases generate a peak at 44.0 ppm that corresponds to the disordered α_d phase and two peaks at 44.7 and 43.8 ppm that are due to the α_2 phase. The two peaks of the α_2 phase are added with the constrained of a 2:1 internal ratio and the same line width. In (a) the peak of the α_d phase is dashed. (ii) The syndiotactic crystalline phases give rise to two peaks with 1:1 intensity ratio at 48.0 and 39.5 ppm for the $s(2/1)s$ helix form and one peak at 49.4 ppm for the extended-chain form.

Table 2. Microstructure Distribution at the Pentad Level in the Sample by Solution NMR and Partitioning of the Stereosequences between the Amorphous and Crystalline Phases at 361 K

	composition by ^{13}C solution NMR	composition by ^{13}C MAS NMR (361 K)	
		molten state	crystalline state (as difference)
<i>mmmm</i>	0.45	0.21	0.24
<i>mmmr</i>	0.08	0.10	~ 0.02
<i>rmrm</i>	0.01	0.01	
<i>rrmm</i>	0.11	0.10	0.01
<i>rrmr + mrrm</i>	0.05	0.05	
<i>rrrm</i>	0	0	0
<i>rrrr</i>	0.20	0.16	0.04
<i>rrrm + mrrm</i>	0.10	0.08	0.02
total amount	1	0.71	0.29

the pentad level of the crystalline phases can be established as the difference between the overall microstructure distribution and the composition of the stereosequences in the "molten state". Only the homotactic pentads (*mmmm* and *rrrr*) are still crystallized at 361 K . The fraction of 0.24 isotactic pentads measured (see Table 2) is in good agreement with the 0.27 fraction of isotactic crystalline phases, as established by MAS NMR and shown in Table 1.

"Annealed PP" Samples. Figure 7a shows the ^{13}C CP MAS NMR methylene spectrum of the "annealed PP" sample, that is cured until $166\text{ }^{\circ}\text{C}$ (see Thermal Behavior section). It can be seen that there is signal

splitting with 2:1 intensity ratio; such splitting is a clear marker of a well-crystallized α_2 isotactic phase that is present here as 75% of the overall crystallinity. The splitting is also in the methine region (not shown). A minor component, reported in Figure 7a as a shadowed area and accounting for 7%, is required to fit the pattern. However, it is not possible to detect this minor component in the methine and methyl region. This minor component is due to the smaller and irregular crystals of disordered α_d phases. Thus, a dramatic reduction of the disordered α_d phase is achieved by high-temperature annealing. For comparison purposes, the spectra of samples containing a larger amount of disorder in the α phase are shown in Figure 7b,c. The latter figure shows the spectrum of a sample heated to the molten state at $190\text{ }^{\circ}\text{C}$ and cooled rapidly: in this case, 34% of the α_d phase signal at 44.0 ppm (due to the high content of disorder) has to be taken into account. This signal causes a change in the maxima and the splitting of the signals in the isotactic region of the spectrum. We have therefore interpreted the spectra as the sum of two contributions: one composed of two peaks at 44.7 and 43.8 ppm with a 2:1 intensity ratio and the other consisting of one resonance at 44.0 ppm . Our interpretation of the spectral profile of the isotactic α phases is based only on the assumption that the balance between the two contributions is determined by the degree of disorder. Deconvolution using just two resonances for the overall isotactic region would imply an assumption of variable chemical shifts of the resonances in each spectrum and a signal intensity ratio with no basis in crystal structure.

Crystallization of the syndiotactic sequences in both the helical form and the extended-chain form occurs in the same amount in all the samples (respectively 14% and 4% of the overall crystallinity). It is reasonable to think that the syndiotactic sequences are already melted at the curing temperature of $160\text{ }^{\circ}\text{C}$, and their crystallization is determined by the cooling process.

The better crystallization of the annealed sample in the α form gives a $T_1(^{13}\text{C})$ values of 53 s and a $T_{1\rho}(^1\text{H})$ relaxation time of 51 ms . The increase in the $T_{1\rho}(^1\text{H})$ value by annealing is due to the larger crystals (about 9 nm),⁴³ as the relaxation times in the hydrogen domain are mostly affected by spin propagation, as already discussed. The syndiotactic sequences crystallize and segregate from the isotactic crystals, as indicated by different $T_{1\rho}(^1\text{H})$ of 18 ms for the syndiotactic crystalline phase (see the above discussion for the "PP" sample). The $T_1(^{13}\text{C})$ relaxation times measured on the peak at 39.4 ppm for the $s(2/1)2$ helix form are as long (50 s) as in the "PP" sample (46 s).

Conclusions

The evident conclusion drawn from these results is that the homotactic sequences of both isotactic and syndiotactic polypropylene are able to crystallize simultaneously in the conformation and crystal arrangements known for homotactic polymers. Moreover, the results highlight the effectiveness of MAS NMR spectroscopy for providing quantitative information and a number of details on the material phase structure even for complex and disordered microstructures. A few allomorphs could be identified in the crystal phases: α_2 and disordered α_d phases for isotactic polypropylene; helix and stretched forms for syndiotactic polypropylene. The allomorphs were quantified as a function of the thermal history.

The overall crystallinity and the partition of the stereosequences between the crystalline and noncrystalline phases could be determined at varying temperatures. At high temperature the mobility of the amorphous phase is high enough to provide the resolution of the stereosequences at the pentad level. Hence, the amounts and microstructure of crystals melting at different temperatures were determined.

Acknowledgment. We thank the PRIN program of MURST and the CNR PF MSTA II project for financial support. S. V. Meille is gratefully thanked for the performance of XRD analysis and helpful discussions. G. Fronza is gratefully acknowledged for the performance of the solution NMR spectrum. C. Scelza is thanked for helpful discussions and S. Di Fiore for technical support.

References and Notes

- Natta, G.; Peraldo, M.; Corradini, P. *Rend., Accad. Naz. Lincei* **1959**, *26*, 14.
- Polypropylene Handbook Polymerization, Characterization, Properties, Processing, Applications*; Moore Jr., E. P., Ed.; Carl Hanser Verlag: Munich, 1996.
- Natta, G.; Corradini, P. *Nuovo Cimento Suppl.* **1960**, *15*, 60.
- Lotz, B.; Wittmann, J. C. *J. Polym. Sci., Part B: Polym. Phys.* **1986**, *24*, 1541.
- Fillon, B.; Wittmann, J. C.; Lotz, B.; Thierry, A. *Polymer* **1993**, *31*, 1383.
- Bunn, A.; Cudby, M. E. A.; Harris, R. K.; Packer, K. J.; Say, B. *J. Polymer* **1982**, *23*, 694.
- Corradini, P.; Napolitano, R.; Oliva, L.; Petraccone, V.; Pirozzi, B.; Guerra, G. *Makromol. Chem., Rapid Commun.* **1982**, *3*, 753.
- Caldas, V.; Morin, F. G.; Brown, G. R. *Magn. Reson. Chem.* **1994**, *32*, S72.
- Huang, T. W.; Alamo, R. G.; Manderlkern, L. *Macromolecules* **1999**, *32*, 6374.
- Keith, H. D.; Padden, F. J., Jr.; Walter, N. M.; Wickoff, H. W. *J. Appl. Phys.* **1959**, *30*, 1485.
- Meille, S. V.; Ferro, D. R.; Brückner, S.; Lovinger, A. J.; Padden, F. J. *Macromolecules* **1994**, *27*, 2615.
- Stocker, W.; Schumacher, M.; Graff, S.; Thierry, A.; Wittmann, J.-C.; Lotz, B. *Macromolecules* **1998**, *31*, 807.
- Gomez, M. A.; Tanaka, H.; Tonelli, A. E. *Polymer* **1987**, *28*, 2227.
- Brückner, S.; Meille, S. V. *Nature* **1989**, *340*, 455.
- Meille, S. V.; Brückner, S.; Porzio, W. *Macromolecules* **1990**, *23*, 4114.
- Brückner, S.; Meille, S. V.; Sozzani, P.; Torri, G. *Makromol. Chem., Rapid Commun.* **1990**, *11*, 55.
- Thomann, R.; Wang, C.; Kressler, J.; Mülhaupt, R. *Macromolecules* **1996**, *29*, 8425.
- Alamo, R. G.; Kim, M.-H.; Galante, M. J.; Isasi, J. R.; Manderlkern, L. *Macromolecules* **1999**, *32*, 4050.
- Lotz, B.; Lovinger, A. J.; Cais, R. E. *Macromolecules* **1988**, *21*, 2375.
- Lovinger, A. J.; Lotz, B.; Davis, D. D.; Padden, F. J. *Macromolecules* **1993**, *26*, 3494.
- Sozzani, P.; Simonutti, R.; Galimberti, M. *Macromolecules* **1993**, *26*, 5782.
- Sozzani, P.; Simonutti, R.; Comotti, A. *Polym. Prepr.* **1996**, *37*, 432.
- Corradini, P.; Natta, G.; Ganis, P.; Temussi, P. A. *J. Polym. Sci., Part C* **1967**, *16*, 2477.
- De Rosa, C.; Auriemma, F.; Vinti, V. *Macromolecules* **1998**, *31*, 7430.
- Natta, G.; Peraldo, M.; Allegra, G. *Makromol. Chem.* **1964**, *75*, 215.
- Chatani, Y.; Maruyama, H.; Noguchi, K.; Asanuma, T.; Shiomura, T. *J. Polym. Sci., Polym. Phys. Lett.* **1990**, *28*, 393.
- Sozzani, P.; Galimberti, M.; Balbontin, G. *Makromol. Chem., Rapid Commun.* **1992**, *13*, 305.
- Sozzani, P.; Simonutti, R.; Comotti, A. *Magn. Reson. Chem.* **1994**, *32*, s45.
- Nakaoki, T.; Ohira, Y.; Hayashi, H.; Horii, F. *Macromolecules* **1998**, *31*, 2705.
- Ohira, Y.; Horii, F.; Nakaoki, T. *Macromolecules* **2000**, *33*, 1801.
- Vittoria, V.; Guadagno, L.; Comotti, A.; Simonutti, R.; Auriemma, F.; De Rosa, C. *Macromolecules* **2000**, *33*, 6200.
- Chatani, Y.; Maruyama, H.; Asanuma, T.; Shiomura, T. *J. Polym. Sci., Part B: Polym. Phys.* **1991**, *29*, 1649.
- Sozzani, P.; Simonutti, R.; Comotti, A. *Macromol. Symp.* **1995**, *89*, 513.
- Sozzani, P.; Simonutti, R. In *Polymeric Materials Encyclopedia*; Polyolefins (Solid State Nuclear Magnetic Resonance); Salamone, J. C., Ed.; CRC Press: Boca Raton, FL, 1996; Vol. 8, pp 6428–6435.
- VanderHart, D. L.; Alamo, R. G.; Nyden, M. R.; Kim, M.-H.; Manderlkern, L. *Macromolecules* **2000**, *33*, 6078.
- Zemke, K.; Chmelka, B. F.; Schmidt-Rohr, K.; Spiess, H. W. *Macromolecules* **1991**, *24*, 6874.
- Torchia, D. A. *J. Magn. Reson.* **1978**, *30*, 613.
- VanderHart, D. L. *J. Chem. Phys.* **1986**, *84*, 1196.
- Krigbaum, W. R.; Uematsu, I. *J. Polym. Sci., Polym. Chem. Ed.* **1965**, *3*, 767.
- Tonelli, A. E. *Macromolecules* **1978**, *11*, 565.
- McBrierty, V. J.; Packer, K. J. *Nuclear Magnetic Resonance in Solid Polymers*; Cambridge University Press: Cambridge, 1993.
- Comotti, A.; Simonutti, R.; Sozzani, P. *Chem. Mater.* **1996**, *8*, 2341.
- In the spin diffusion regime the phase dimensions were evaluated considering that the distance covered by the propagation of magnetization follows the formula $\langle L^2 \rangle = 6D\tau$ where D is the diffusion coefficient. D is 6.2×10^{-16} m²/s in the laboratory frame for the polyethylene (the proton density is equal in both polyethylene and polypropylene). In the presence of a spin-lock field along the x axis, D is half that value, since spin-diffusion constants are proportional to $(3 \cos^2 \theta - 1)$.
- Tanaka, H.; Fujiwara, Y.; Asano, T. *Makromol. Chem.* **1993**, *194*, 2279.

MA002146O